

Quantum origin of inflation in the geometric inflation model

Israel Quiros^{1,*}, Roberto De Arcia^{2,†}, Ricardo García-Salcedo^{1,3,‡}, Tame Gonzalez^{1,§},
Francisco X. Linares Cedeño^{4,5,||} and Ulises Nucamendi^{4,6,¶}

¹*Departamento Ingeniería Civil, División de Ingeniería, Universidad de Guanajuato, Guanajuato CP 36000, México*

²*Departamento de Astronomía, División de Ciencias Exactas, Universidad de Guanajuato, Guanajuato CP 36240, México*

³*CICATA-Legaria, Instituto Politécnico Nacional, Ciudad de México CP 11500, México*

⁴*Instituto de Física y Matemáticas, Universidad Michoacana de San Nicolás de Hidalgo, Edificio C-3, Ciudad Universitaria, CP 58040 Morelia, Michoacán, México*

⁵*Mesoamerican Centre for Theoretical Physics, Universidad Autónoma de Chiapas, Carretera Zapata Km 4, Real del Bosque (Terán), 29040 Tuxtla Gutiérrez, Chiapas, México*

⁶*Departamento de Física, Cinvestav, Avenida Instituto Politécnico Nacional 2508, San Pedro Zacatenco 07360, Gustavo A. Madero, Ciudad de México, México*



(Received 18 July 2020; accepted 3 March 2021; published 22 March 2021)

In this paper we investigate the cosmological dynamics of geometric inflation by means of the tools of the dynamical systems theory. We focus on the study of two explicit models where it is possible to sum the infinite series of higher curvature corrections that arise in the formalism. These would be very interesting possibilities since, if we regard gravity as a quantum effective theory, a key feature is that higher powers of the curvature invariants are involved at higher loops. Hence, naively, consideration of the whole infinite tower of curvature invariants amounts to consideration of all of the higher-order loops. The global dynamics of these toy models in the phase space is discussed and the quantum origin of primordial inflation is exposed.

DOI: [10.1103/PhysRevD.103.064043](https://doi.org/10.1103/PhysRevD.103.064043)

I. INTRODUCTION

Since long ago it has been suggested that the quantum gravity action should contain, in addition to the Einstein-Hilbert action, contributions from higher-order curvature invariants involving more than the first two derivatives of the metric tensor [1]. Although such higher-derivative terms in the action would carry negligible consequences in the classical (infrared) domain, at high frequencies they would dominate, leading to power-counting renormalization [2,3]. It has been shown that gravitational actions which include terms quadratic in the curvature tensor are indeed renormalizable, although not unitary [4]. After due consideration of the Gauss-Bonnet (GB) invariant,

$$\mathcal{G} = R^2 - 4R_{\mu\nu}R^{\mu\nu} + R_{\mu\nu\lambda\sigma}R^{\mu\nu\lambda\sigma}, \quad (1)$$

only terms $\propto R^2$ and $\propto R_{\mu\nu}R^{\mu\nu}$ were considered in [4]. As shown in [5] (see also [6,7]) such a quadratic (two-parametric) class of theories yields to a class of multimass

models of gravity with a total of eight degrees of freedom; in addition to the usual massless excitations of the field (two degrees of freedom), there are now massive spin-two (five degrees of freedom) and massive scalar excitations. The massive spin-two part of the field has negative energy so that it is a ghost excitation which for an effective theory could not be catastrophic, but from a quantum perspective leads to nonunitarity.

In four-dimensional space the class of theories derivable from Lagrangians that depend exclusively on the metric tensor field $\mathcal{L} = \mathcal{L}(g_{\mu\nu})$ (and on its derivatives), and that admit second-order equations of motion, are limited by the Lovelock theorem [8,9]. According to this theorem, the only second-order Euler-Lagrange equation $\mathcal{E}_{\mu\nu} = 0$ obtainable in a four-dimensional space from a Lagrangian of the form $\mathcal{L}(g_{\mu\nu})$ is when [10] $\mathcal{E}_{\mu\nu} = \sqrt{|g|}(\alpha G_{\mu\nu} + \lambda g_{\mu\nu})$, where α and λ are constants and $G_{\mu\nu} = R_{\mu\nu} - g_{\mu\nu}R/2$ is the Einstein tensor. The general class of Lagrangians that lead to these second-order equations of motion read:

$$\mathcal{L} = \sqrt{|g|}(\alpha R + \beta \mathcal{G}) + \gamma \epsilon^{\mu\nu\sigma\lambda} R^{\alpha\beta}_{\mu\nu} R_{\alpha\beta\sigma\lambda},$$

where the second and third terms above do not contribute to the Euler-Lagrange equations. As a consequence, in four dimensions the only viable alternatives to general

*iquiros@fisica.ugto.mx
†robertodearcia@gmail.com
‡rigarcias@ipn.mx
§tamegc72@gmail.com
||francisco.linares@umich.mx
¶unucamendi@gmail.com

relativity (GR) should be based either (i) on the consideration of other fields beyond the metric, (ii) on the assumption of higher-dimensional spaces, or (iii) on the inclusion of higher than second-order derivatives of the metric in the equations of motion, among a few others [10].

Hence, an interesting possibility to evade the Lovelock theorem in order to obtain equations of motion that differ from the GR ones is to relax the requirement of considering up to second-order derivatives of the metric. This has been, precisely, the route followed in a series of recent works [11–17] in order to obtain dynamics substantially different from those resulting from GR.

Among these “beyond Lovelock” proposals is the so called Einsteinian cubic gravity (ECG) theory [11–13]. The ECG formalism is the outcome of an approach based on a D -dimensional theory involving arbitrary contractions of the Riemann tensor and the metric

$$S = \int d^D x \sqrt{|g|} \mathcal{L}(g_{\mu\nu}, R_{\mu\nu\sigma\lambda}), \quad (2)$$

whose motion equation is

$$\mathcal{E}_{\mu\nu} = P_{\mu\sigma\rho\lambda} R_{\nu}^{\sigma\rho\lambda} - \frac{1}{2} g_{\mu\nu} \mathcal{L} - 2\nabla^\lambda \nabla^\sigma P_{\mu\lambda\sigma\nu} = 0, \quad (3)$$

where $\mathcal{E}_{\mu\nu}$ is the Euler-Lagrange tensor, and

$$P^{\mu\nu\sigma\lambda} \equiv \left. \frac{\partial \mathcal{L}}{\partial R_{\mu\nu\sigma\lambda}} \right|_{g_{\alpha\beta}},$$

contains up to fourth-order derivatives of the metric. The linearization of (3) around maximally symmetric backgrounds¹ with the Riemann tensor

$$R_{\mu\nu\sigma\lambda}^{(0)} = \Lambda [g_{\mu\sigma} g_{\lambda\nu}^{(0)} - g_{\mu\lambda}^{(0)} g_{\sigma\nu}^{(0)}],$$

yields to the gravitational spectrum consisting of (i) a massless graviton, and (ii) a massive (ghost) graviton with mass m_g and a massive scalar mode with mass m_s , i.e., basically the same spectrum found in the four-dimensional quadratic theory of [4–7] (for the full details of the linearization procedure see [11]). In the effective theory, in the limit $|m_g| \rightarrow \infty$, $|m_s| \rightarrow \infty$, the massive vacuum modes become infinitely heavy and decouple from the spectrum of the theory, leaving the massless graviton as the only propagating vacuum degree of freedom, as in GR. It is demonstrated in [11] that the most general cubic theory possessing dimension-independent couplings, which shares the spectrum with GR, reads:

¹The metric gets small perturbations of the kind $g_{\mu\nu} = g_{\mu\nu}^{(0)} + h_{\mu\nu}$, where $g_{\mu\nu}^{(0)}$ is the background metric while $h_{\mu\nu} \ll 1$ are small perturbations.

$$\mathcal{L} = \frac{\sqrt{|g|}}{2} (R - 2\Lambda_0 + 2\alpha\mathcal{G} + 2\beta\mathcal{T}_{(3)} + 2\lambda\mathcal{P}), \quad (4)$$

where, in four dimensions, the GB term \mathcal{G} amounts to a total derivative, while the cubic Lovelock term $\mathcal{T}_{(3)}$ identically vanishes. The cubic term \mathcal{P} ,

$$\mathcal{P} = 12R_{\mu}^{\nu}{}_{\lambda}{}^{\sigma} R_{\nu}{}^{\tau}{}_{\sigma}{}^{\rho} R_{\tau}{}^{\mu}{}_{\rho}{}^{\lambda} + R_{\mu\lambda}{}^{\nu\sigma} R_{\nu\sigma}{}^{\tau\rho} R_{\tau\rho}{}^{\mu\lambda} - 12R_{\mu\lambda\nu\sigma} R^{\mu\nu} R^{\lambda\sigma} + 8R_{\mu}{}^{\lambda} R_{\lambda}{}^{\nu} R_{\nu}{}^{\mu}, \quad (5)$$

is neither trivial nor topological in four dimensions.

In [15] a cubic modification of Einstein’s GR was proposed which generalizes the ECG theory [11,12,14]. The proposed modification, called cosmological ECG (CECG) theory, rests on the following combination of cubic invariants: $\mathcal{P} - 8\mathcal{C}$, where

$$\mathcal{C} = R_{\mu\lambda\nu\sigma} R^{\mu\lambda\nu}{}_{\tau} R^{\sigma\tau} - \frac{1}{4} R R_{\mu\lambda\nu\sigma} R^{\mu\lambda\nu\sigma} - 2R_{\mu\lambda\nu\sigma} R^{\mu\nu} R^{\lambda\sigma} + \frac{1}{2} R R_{\mu\nu} R^{\mu\nu}. \quad (6)$$

Although this latter invariant was previously found in [13], in that reference the authors were interested in static spherically symmetric spaces where \mathcal{C} vanishes. The action of the CECG theory and the derived equations of motion read (we adopt $\mathcal{R}_{(3)} \equiv \mathcal{P} - 8\mathcal{C}$):

$$S = \frac{1}{2} \int d^4 x \sqrt{|g|} (R - 2\Lambda + 2\beta\mathcal{R}_{(3)}),$$

$$2\mathcal{E}_{\mu\nu} = G_{\mu\nu} + g_{\mu\nu}\Lambda + 2\beta \left[\left(\frac{\partial \mathcal{R}_{(3)}}{\partial R^{\mu\alpha\beta\sigma}} \right) R_{\nu}^{\alpha\beta\sigma} - \frac{1}{2} g_{\mu\nu} \mathcal{R}_{(3)} - 2\nabla^\alpha \nabla^\beta \left(\frac{\partial \mathcal{R}_{(3)}}{\partial R^{\mu\alpha\beta\nu}} \right) \right] = 0. \quad (7)$$

In general, the Eqs. (7) are fourth-order and so the Lovelock theorem [8] is not violated by the CECG theory. An interesting property of this theory is that in Friedmann-Robertson-Walker (FRW) spacetime the motion equations are second-order in the time derivatives. For other backgrounds such as, for instance, the plane-symmetric Bianchi I space, the cosmological equations are fourth-order in the derivatives (see Appendix A of [18]).

In [16], it is shown that the combination of cubic invariants defining five-dimensional quasitopological gravity, when written in four dimensions, reduces to the CECG theory. It also introduced a quartic version of the CECG theory and a combination of quintic invariants with the properties of the mentioned theory. In [19], the effect of higher-curvature terms in the string low-energy effective action has been studied for the bosonic and heterotic strings, as well as for the type II superstring in the cosmological context, up to quartic corrections in the

curvature invariants.² Meanwhile, in [17] it is shown how to construct invariants up to eighth-order in the curvature. In the latter reference it was also shown that the presence of an inflationary epoch is a natural, almost unavoidable, consequence of the existence of a sensible formalism involving an infinite tower of higher-curvature corrections to the Einstein-Hilbert action. The formalism was called “geometric inflation” because the only field required was the metric. In string theory we are familiar with such a structure as the string effective action contains an infinite series of higher curvature corrections to the leading Einstein gravity (see, for instance, [19]).

The beyond Lovelock theories—as any other higher curvature modification of GR—are characterized by the high complexity of their mathematical structure, so that only through feasible approximations may one retrieve some useful analytic information on the cosmological dynamics. Otherwise, one has to perform either a numeric investigation or apply the tools of the dynamical systems theory. The latter allows one to retrieve very useful information on the asymptotic dynamics of the mentioned cosmological models. The asymptotic dynamics may be characterized by either (i) attractor solutions to which the system evolves for a wide range of initial conditions, (ii) saddle equilibrium configurations that attract the phase space orbits in one direction but repel them in another direction, (iii) source critical points which may be pictured as past attractors, or (iv) limit cycles, among others. Although the use of the dynamical systems is especially useful when one deals with scalar-field cosmological models (for a small but representative sample see [21–27]), its usefulness in other contexts has been explored as well [28–31]. The tools of the dynamical systems have been used, in particular, in the study of the CECG cosmological model in [32], while in [33] the dynamics of the so-called extended cubic gravity, $f(\mathcal{P})$, was explored.

As stated above, in [32] the cosmological dynamics of an up-to-cubic curvature correction to GR—known as CECG theory—was investigated. It was confirmed that an inflationary matter-dominated big bang was the global past attractor, which means that inflation is the starting point of any physically meaningful cosmic history in that set up. However, as discussed in [18], certain instabilities may be present in this purely cubic model. In this regard it could be very interesting to explore how the results of [32] are modified when all orders of curvature are included, in particular because such a configuration could avoid the kind of instabilities found in [18] in the CECG model.

In the present paper we shall look for the global asymptotic dynamics of the geometric inflation formalism developed in [17], which considers the whole infinite tower of higher curvature corrections to GR. We shall explore two

explicit toy models where it is possible to sum the infinite series of higher curvature corrections that arise in the formalism. Including all orders of curvature would be a very interesting possibility. Besides, if we regard gravity as a quantum effective theory [34], it is a well-behaved quantum theory at low energies. For the gravitational part of the effective theory we would have

$$S_{\text{eff}} = \int \frac{d^4x \sqrt{|g|}}{2} (R - 2\Lambda + c_1 R^2 + c_2 R_{\mu\nu} R^{\mu\nu} + \dots),$$

where Λ , c_1 , and c_2 are constants and the ellipses denote higher powers of R , $R_{\mu\nu}$, and $R_{\mu\nu\sigma\lambda}$. At one loop the divergences due to the massless gravitons read [2]:

$$\Delta\mathcal{L}^{(1)} = \frac{1}{8\pi^2\epsilon} \left(\frac{1}{120} R^2 + \frac{7}{20} R_{\mu\nu} R^{\mu\nu} \right),$$

where the constant $\epsilon = 4 - d$ within dimensional regularization (recall that we work with units where $8\pi G_N = 1$). At two loops these divergences have the form [35]

$$\Delta\mathcal{L}^{(2)} = \frac{209}{1440(16\pi^2)^2\epsilon} R^{\alpha\beta}{}_{\mu\nu} R^{\mu\nu}{}_{\sigma\lambda} R^{\sigma\lambda}{}_{\alpha\beta}.$$

As properly noted in [34], the key feature is that higher powers of R , $R_{\mu\nu}$, and $R_{\mu\nu\sigma\lambda}$ are involved at higher loops. In this regard the two toy models proposed in [17] would represent an interesting possibility to consider all of the higher-order modifications of GR, i.e., all of the higher-order graviton loops, without involving a perturbative approach. One would naively expect that consideration of the whole infinite tower of curvature invariants would amount to consideration of all of the higher-order loops. Hence, quantum effects would be manifest at the high curvature regime, at least.

Our aim is to corroborate, from the dynamical systems perspective, the result of [17]—that primordial inflation is a generic outcome of the resulting cosmological model. While doing so, the role of the new scale, $L \gtrsim L_{\text{Pl}}$ (L_{Pl} is the Planck length), will be revealed as well. We will be able to connect the inflationary stage with the effects that arise at curvature scales $\sim L_{\text{Pl}}^{-2} \gtrsim L^{-2}$, so that these are necessarily quantum effects. We shall show that in the “classic limit”, i.e., in the limit when the coupling of the higher curvature corrections vanishes, the primordial inflation of quantum origin is replaced by a big bang singularity. As far as we know, the global cosmological dynamics of the above mentioned models have not been investigated before.

We have organized the paper in the following way. In Sec. II, the basic elements of the geometric inflation formalism are given. In Sec. III, we expose the main properties of the dynamical system corresponding to the two toy models proposed in [17], where the sum of the infinite tower of higher curvature corrections to gravity is

²In the context of superstring theory it has been shown long ago that the effective gravitational action should be, at least, 4th order in the Riemann tensor [20].

explicitly computed. The global dynamics of the mentioned toy models are discussed in Sec. IV, where the results of the dynamical systems study are presented and physically analyzed. In Sec. V we discuss the physical consequences of the obtained results, while brief conclusions are given in Sec. VI. Unless stated otherwise, here we use the units where $8\pi G_N = M_{\text{Pl}}^{-2} = c^2 = 1$ (M_{Pl} is the reduced Planck mass).

II. THE BASICS OF THE GEOMETRIC INFLATION FORMALISM

Here we consider the formalism proposed in [17] that relies on the following action:

$$S = \int \frac{d^4x \sqrt{|g|}}{2} \left[R - 2\Lambda + \sum_{n=3}^{\infty} \lambda_n L^{2n-2} \mathcal{R}_{(n)} \right], \quad (8)$$

where $\mathcal{R}_{(n)}$ are densities constructed from contractions of the metric and the Riemann tensor, λ_n are dimensionless constants, and L^{-1} is a new energy scale below the Planck scale $L^{-1} \lesssim L_{\text{Pl}}^{-1}$. For $L^{-1} \ll L_{\text{Pl}}^{-1}$ (and $\lambda_3 \neq 0$), the theory is affected by causality issues due to the presence of an infinite tower of massive higher spin particles [36]. Besides, as stated in [17], the most reasonable choice for the new scale L^{-1} seems to be that it corresponds to some new scale below the Planck mass, but high enough to make the higher-curvature effects become negligible at late times. Here, in line with the former analysis, we shall assume that $L^{-1} \lesssim L_{\text{Pl}}^{-1}$.

Among other desirable properties, the geometric inflation theory is ghost-free around maximally symmetric backgrounds and the FRW cosmological equations of motion are second-order, such as these are for the CECG theory [15]. Actually, in terms of the FRW line-element with flat spatial sections,

$$ds^2 = -dt^2 + a^2(t) \delta_{ik} dx^i dx^k.$$

The cosmological equations of motion derived from (8) with the addition of a matter piece of action read [17]:

$$\begin{aligned} 3F(H) &= \rho_m + \Lambda, \\ \frac{\dot{H}}{H} F'(H) &= -(p_m + \rho_m), \\ \dot{\rho}_m &= -3H(\rho_m + p_m), \end{aligned} \quad (9)$$

where H is the Hubble parameter, ρ_m and p_m are the energy density and pressure of the matter fluid,³ and $F' \equiv dF/dH$. The function $F = F(H)$ reads:

³In what follows, for simplicity, we assume the following equation of state (EOS) for the matter fluid: $p_m = \omega_m \rho_m$, where the constant ω_m is the EOS parameter.

$$F(H) = H^2 + L^{-2} \sum_{n=3}^{\infty} (-1)^n \lambda_n (LH)^{2n}. \quad (10)$$

As appropriately discussed in [17], there is an ambiguity in the choice of the coefficients λ_n in (8) which is linked to a similar ambiguity that has been discussed long ago within the context of string theory [37–42] (see the related discussion in the final paragraphs of Sec. V). The ambiguity can be stated in the following way: Suppose that $\mathcal{R}_{(n)}$ and $\mathcal{R}'_{(n)}$ are two different densities such that

$$\mathcal{R}_{(n)} = \mathcal{R}'_{(n)} + \mathcal{T}_{(n)},$$

where the density $\mathcal{T}_{(n)}$ does not affect the equations of motion in four dimensions.⁴ Hence, the action

$$\begin{aligned} S' &= \int \frac{d^4x \sqrt{|g|}}{2} \left[R - 2\Lambda + \sum_{n=3}^{\infty} \lambda'_n L^{2n-2} \mathcal{R}'_{(n)} \right] \\ &= \int \frac{d^4x \sqrt{|g|}}{2} \left[R - 2\Lambda + \sum_{n=3}^{\infty} \lambda'_n L^{2n-2} \mathcal{R}_{(n)} \right], \end{aligned}$$

where the constants $\lambda'_n \neq \lambda_n$ and (8) are equivalent actions. This means that (at least) one or several of the dimensionless constants λ_n can be arbitrarily chosen. In this regard, in Ref. [17] two different kinds of conditions were given on the dimensionless parameters λ_n such that the infinite summation in (10) can be explicitly performed⁵: $\lambda_{2k+1} = 0$, $\lambda_{4+2k} = \lambda_4/k!$ (k is a positive integer) for model 1 and $\lambda_3 > 0$, $\lambda_{n \geq 4} = (-1)^n \lambda_3/(n-4)!$ for model 2. These conditions led to two different toy models that are based in the following forms of the function F :

$$F(H) = H^2 [1 + \lambda_4 (LH)^6 e^{(LH)^4}], \quad (11)$$

for model 1 and

$$F(H) = H^2 \{1 - \lambda_3 (LH)^4 [1 - (LH)^2 e^{(LH)^2}]\}, \quad (12)$$

for model 2, respectively. Since in these models it is possible to sum over the infinite tower of higher-order curvature contributions, we expect that at high curvature $H^2 \gtrsim L^{-2}$ quantum gravitational effects would become important, if the present classical theory is regarded as

⁴An example is

$$\begin{aligned} \mathcal{T}_{(3)} &= R_{\mu\nu\sigma\lambda} R^{\mu\nu\sigma\tau} R^{\lambda\tau} - \frac{1}{2} (R_{\mu\nu\sigma\lambda} R^{\mu\nu\sigma\lambda} R + R^3) \\ &\quad + 2(R_{\mu\nu} R^{\mu\nu} R - R_{\mu\nu\sigma\lambda} R^{\mu\sigma} R^{\nu\lambda} - R^{\mu\nu} R_{\nu\sigma} R_{\mu}^{\sigma}), \end{aligned}$$

which vanishes in four dimensions [16].

⁵As clearly stated in [17] many other summable choices are possible.

an effective quantum theory [34]. As a matter of fact, the Planck length represents the boundary of the quantum domain, so that below L_{Pl} , i.e., at very high curvature $H^2 \gtrsim L_{\text{Pl}}^{-2}$, quantum gravity is the dominating contribution. Strictly speaking, we would trust the present formalism up to curvatures $\sim L_{\text{Pl}}^{-2}$.

III. THE DYNAMICAL SYSTEM

Here we follow quite a different approach than in [32]. We choose variables of some phase space that are dimensionless and bounded as in the mentioned reference, but the constants of the theory λ_k , where $k = 4$ for model 1 while $k = 3$ for model 2, are not absorbed into these variables. Instead these remain free constants of the dynamical system, affecting the existence and stability of the equilibrium configurations.

A. Model 1

The cosmological equations of motion (9) for the choice (11) read:

$$1 + \lambda_4 L^6 H^6 e^{L^4 H^4} = \Omega_m + \Omega_\Lambda, \quad (13)$$

$$-2 \frac{\dot{H}}{H^2} = \frac{3(\omega_m + 1)\Omega_m}{1 + 2\lambda_4 L^6 H^6 e^{L^4 H^4} (2 + L^4 H^4)},$$

where, as customary, $\Omega_m \equiv \rho_m/3H^2$ is the dimensionless energy density of the matter degrees of freedom, while $\Omega_\Lambda = \Lambda/3H^2$.

Here, in order to investigate the global asymptotic dynamics of this model, we introduce the following bounded variables of some phase space:

$$x \equiv \frac{1}{1 + L^2 H^2} \Rightarrow L^2 H^2 = \frac{1-x}{x},$$

$$y \equiv \frac{1}{1 + \Omega_m} \Rightarrow \Omega_m = \frac{1-y}{y}, \quad (14)$$

where $0 \leq x \leq 1$ and $0 \leq y \leq 1$. The modified Friedmann constraint—the first equation in (13)—can be written in the following way:

$$\Omega_\Lambda = \frac{2y-1}{y} + \frac{\lambda_4(1-x)^3 e^{(\frac{1-x}{x})^2}}{x^3}. \quad (15)$$

Meanwhile,

$$\frac{\dot{H}}{H^2} = -\frac{3(\omega_m + 1)x^2 A(x)(1-y)}{2B(x)y}, \quad (16)$$

where, for compactness of writing, we have introduced the functions

$$A(x) = x^3 e^{-(\frac{1-x}{x})^2},$$

$$B(x) = x^5 e^{-(\frac{1-x}{x})^2} + 2\lambda_4(1-x)^3(3x^2 - 2x + 1), \quad (17)$$

respectively.

In terms of the phase space variables x, y , the second-order cosmological equations (9) may be traded by the following two-dimensional autonomous dynamical system:

$$\frac{dx}{dv} = \frac{3(\omega_m + 1)x^3(1-x)A(x)(1-y)}{B(x)},$$

$$\frac{dy}{dv} = 3(\omega_m + 1)y(1-y) \left[y - \frac{x^2 A(x)(1-y)}{B(x)} \right], \quad (18)$$

where we have introduced the time variable

$$v = \int (1 + \Omega_m) H dt. \quad (19)$$

The phase space to look for equilibrium configurations of the dynamical system (18) is the following unit phase square:

$$\Psi = \{(x, y) : 0 \leq x \leq 1, 0 \leq y \leq 1\}. \quad (20)$$

The separatrix

$$S = \{(x, y) : 0 \leq x \leq 1, y = \bar{y}_1(x)\}, \quad (21)$$

where

$$\bar{y}_1(x) = \frac{A(x)}{2A(x) + \lambda_4(1-x)^3}, \quad (22)$$

separates the region where the background space is de Sitter, $\Omega_\Lambda \geq 0 \Rightarrow y \geq \bar{y}_1(x)$, from the region where the background space is anti-de Sitter, $\Omega_\Lambda < 0 \Rightarrow y < \bar{y}_1(x)$. Here we concentrate on de Sitter background spaces exclusively, so we shall consider only the region of the phase square above the separatrix:

$$\Psi_{\text{phys},1} = \{(x, y) : 0 \leq x \leq 1, \bar{y}_1(x) \leq y \leq 1\}. \quad (23)$$

Another curve of physical interest is the one related with the change of sign of the deceleration parameter:

$$q \equiv -1 - \frac{\dot{H}}{H^2}, \quad (24)$$

i.e., the curve that follows from the condition $q = 0$,

$$\hat{y}_1(x) = \frac{3(\omega_m + 1)x^2 A(x)}{3(\omega_m + 1)x^2 A(x) + 2B(x)}. \quad (25)$$

Accelerated expansion occurs whenever $y > \hat{y}_1(x)$.

B. Model 2

Here, as in the former subsection, we shall focus in de Sitter background spaces exclusively, so that only the case with $\Lambda \geq 0$ will be of interest. The cosmological equations of motion (9) for the choice (12) read:

$$1 - \lambda_3 L^4 H^4 + \lambda_3 L^6 H^6 e^{L^2 H^2} = \Omega_m + \Omega_\Lambda,$$

$$\frac{\dot{H}}{H^2} = \frac{-3(\omega_m + 1)\Omega_m/2}{1 - 3\lambda_3 L^4 H^4 + \lambda_3(4 + L^2 H^2)L^6 H^6 e^{L^2 H^2}},$$

$$\dot{\Omega}_m = -H\Omega_m \left[3(\omega_m + 1) + 2\frac{\dot{H}}{H^2} \right], \quad (26)$$

where λ_3 is a dimensionless coupling constant and, as before, $\Omega_m \equiv \rho_m/3H^2$ while $\Omega_\Lambda = \Lambda/3H^2$.

We shall use the same variables (14). We get that

$$\Omega_\Lambda = \frac{2y-1}{y} - \lambda_3 \left(\frac{1-x}{x} \right)^2 \left[1 - \left(\frac{1-x}{x} \right) e^{\frac{1-x}{x}} \right], \quad (27)$$

and

$$\frac{\dot{H}}{H^2} = -\frac{3(\omega_m + 1)x^4(1-y)}{2D(x)y}, \quad (28)$$

where we have introduced the functions

$$C(x) = 3x^2 - (1+3x)(1-x)e^{\frac{1-x}{x}},$$

$$D(x) = x^4 - \lambda_3(1-x)^2 C(x). \quad (29)$$

The following ordinary differential equations (ODEs) are obtained out of (14) and (26):

$$x' = -2x(1-x)\frac{\dot{H}}{H^2},$$

$$y' = y(1-y) \left[3(\omega_m + 1) + 2\frac{\dot{H}}{H^2} \right],$$

where the prime denotes derivative with respect to the time variable, $\tau = \ln a$. In a more explicit form, the above equations can be written as follows:

$$\frac{dx}{dv} = \frac{3(w_m + 1)x^5(1-x)(1-y)}{D(x)},$$

$$\frac{dy}{dv} = 3(w_m + 1)y(1-y) \left[y - \frac{x^4(1-y)}{D(x)} \right], \quad (30)$$

where we have used the time variable v in (19), instead of $\tau = \int H dt$. Notice that under the replacement $D(x) \rightarrow x^2 B(x)/A(x)$, i.e.,

$$\lambda_3 \rightarrow 2\lambda_4 \frac{(3x^2 - 2x + 1)e^{\left(\frac{1-x}{x}\right)^2}}{(3x^2 - 2x - 1)e^{\left(\frac{1-x}{x}\right)} - 3x^2}, \quad (31)$$

the dynamical system (18) transforms into (30), so that these are mathematically equivalent. This means, in turn, that the global dynamics of both models share the same features.

Since here we consider de Sitter background spaces exclusively, $\Omega_\Lambda \geq 0$, then from (27) it follows that the physically meaningful region of the phase space, $\Psi = \{(x, y) : 0 \leq x \leq 1, 0 \leq y \leq 1\}$, is the one located above the separatrix $y = \bar{y}_2(x)$, where

$$\bar{y}_2(x) = \frac{x^3}{2x^3 - \lambda_3(1-x)^2[x - (1-x)e^{\frac{1-x}{x}}]}, \quad (32)$$

i.e.,

$$\Psi_{\text{phys},2} = \{(x, y) : 0 \leq x \leq 1, \bar{y}_2(x) \leq y \leq 1\}. \quad (33)$$

Accelerated expansion occurs for points above the curve $y = \hat{y}_2(x)$:

$$\hat{y}_2(x) = \frac{3(w_m + 1)x^4}{3(w_m + 1)x^4 + 2D(x)}. \quad (34)$$

IV. GLOBAL DYNAMICS OF THE MODELS

The fact that in the models (11) and (12) it is possible to sum over the infinite tower of higher-order curvature corrections in (10) means that geometric manifestation of quantum effects is possible in these models. One may reach the same conclusion if they regard the geometric inflation formalism as a quantum effective theory [34]. If this were so, then these effects should be reflected in the properties of the phase space, including its equilibrium configurations. One would expect, in particular, that the inflationary behavior in the models would be strongly correlated with quantum effects. Our expectations are confirmed by the investigation of the global dynamics of the models, as we shall see.

Before we list the critical points of the dynamical systems corresponding to the above models and expose their main properties, we want to briefly discuss an important issue in connection with the existence of an inflationary quantum manifold in the phase space of the models, as it is revealed by the numerical investigation. Here we assume that this manifold is located within the quantum domain, or trans-Planckian region of phase space, where $H^2 > L_{\text{Pl}}^{-2}$ (below we shall discuss supporting arguments). One related question is how to identify where the Planck scale $H^2 = L_{\text{Pl}}^{-2}$ is located in the phase square. One expects that within the theory (8) one may find, at least, an estimate of the magnitude of the new scale L^{-1} , so that the ratio

$$\alpha = \frac{L^2}{L_{\text{Pl}}^2}, \quad (35)$$

should be fixed by the theory itself. Instead, what we have is a very rough lower bound [17]: $\alpha \gtrsim 1$. In the absence of a more accurate estimate one may identify other possible clues of where to locate the x -position in the phase plane where $H^2 = L_{\text{Pl}}^{-2}$. Given the definition of the phase space variable x (14),

$$x = \frac{1}{1 + L^2 H^2}, \quad (36)$$

the origin $x = 0$ is linked with the condition $H^2 \gg L^{-2}$ and, since in the present models we assume that $L^{-2} \lesssim L_{\text{Pl}}^{-2}$,

then $H^2 \gg L_{\text{Pl}}^{-2}$ as well. Meanwhile, the new scale L is located at $H^2 = L^{-2} \rightarrow x = 1/2$ (the vertical dash-dot line that splits the phase portraits in Figs. 1 and 2 into two halves). This means that the Planck scale may be located somewhere between $x = 0$ and $x = 1/2$ in the phase square. From (36) it follows that at $H^2 = L_{\text{Pl}}^{-2}$,

$$x_{\text{Pl}} = \frac{1}{1 + L^2/L_{\text{Pl}}^2} \rightarrow L_{\text{Pl}}^{-2} = \left(\frac{1 - x_{\text{Pl}}}{x_{\text{Pl}}} \right) L^{-2}, \quad (37)$$

where x_{Pl} marks the position of the Planck scale (also the quantum boundary) in the phase plane. Substituting (35) into the left equation of (37) one obtains that

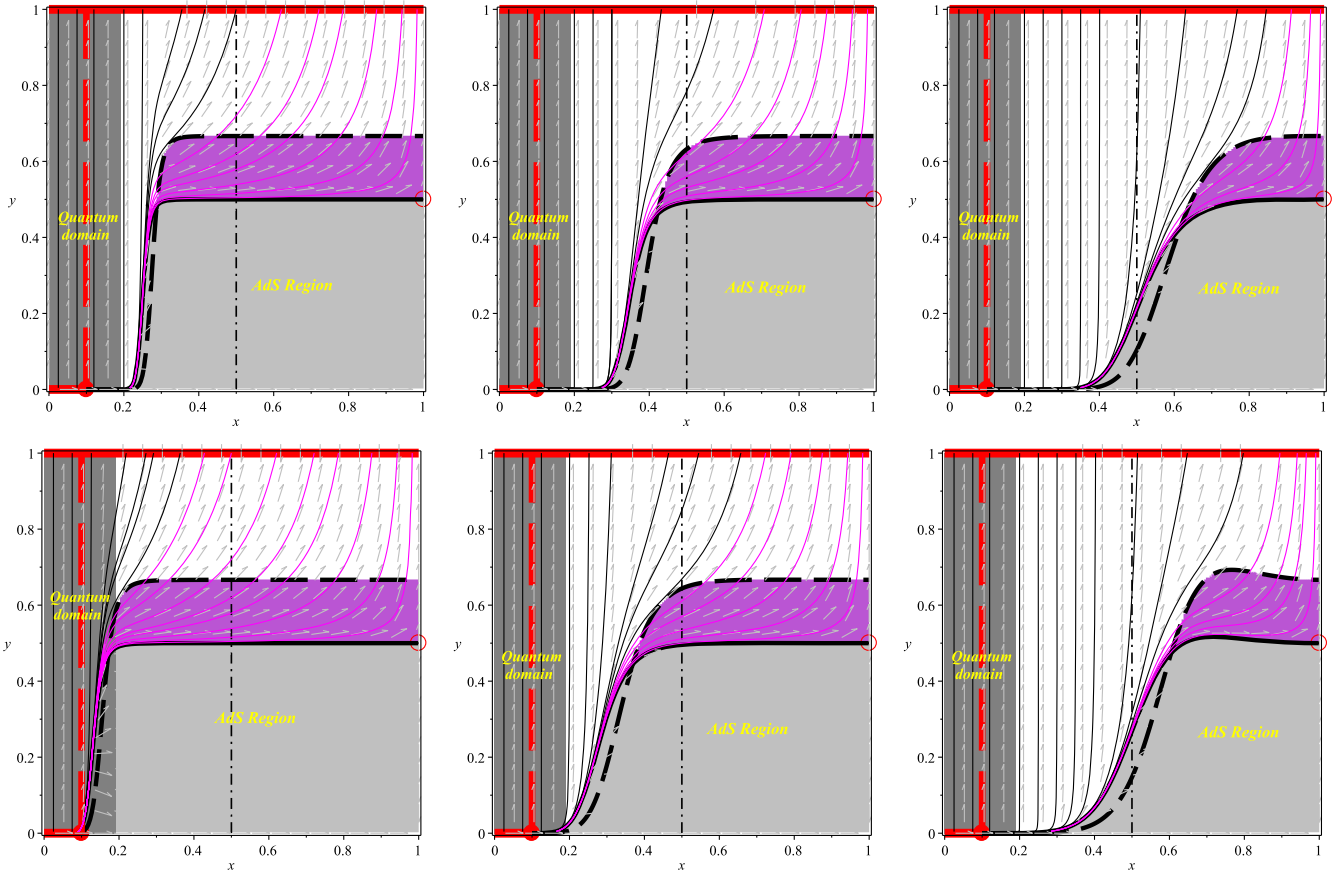


FIG. 1. Phase portraits of the dynamical systems for models 1 and 2 (top and bottom panels, respectively) for the radiation ($\omega_m = 1/3$). Different choices of the dimensionless constants λ_k ($k = 4$ for model 1 and $k = 3$ for model 2) are considered. From left to right: (i) $\lambda_k = 10^{-5}$, (ii) $\lambda_k = 10^{-2}$, and (iii) $\lambda_k = 1$. The critical point $P_{\text{mat}} : (1, 1/2)$ is enclosed by the small circle, while the de Sitter critical manifold \mathcal{M}_{dS} is represented by the thick solid (red) horizontal line coincident with the upper boundary. The quantum inflationary manifold, $\mathcal{Q}_{\text{infl}} = \{(x, 0) : 0 \leq x \leq \langle x \rangle\}$, is represented by the thick solid (red) horizontal segment at $y = 0$ (lower boundary), that starts at the origin and ends up at the solid circle representing the averaged value $\langle x \rangle$, at which $H = L_{\text{Pl}}^{-1}$ (thick vertical long-dash red line). The quantum domain, which includes the fuzzy boundary around $\langle x \rangle$ is represented by the vertical (dark gray) strip with thickness $d \sim |\delta_\sigma x|$, where according to (50): $|\delta_\sigma x| \sim \langle x \rangle (1 - \langle x \rangle)$. The vertical dash-dot straight line that splits the phase portraits into two halves represents the points where $H = L^{-1}$. The separatrix S (dark curve) and the curve corresponding to the condition $q = -1 - \dot{H}/H^2 = 0$ (dark dashed curve) are also shown. The region above the separatrix is for the de Sitter background ($\Omega_\Lambda > 0$) while the region below it (gray shading) corresponds to anti-de Sitter background space, which is not of interest here. Above the dashed curve the expansion occurs at an accelerated pace while below it the cosmic expansion is decelerated. The orbits that meet the region with decelerated expansion (magenta shading) are drawn same color as the region.

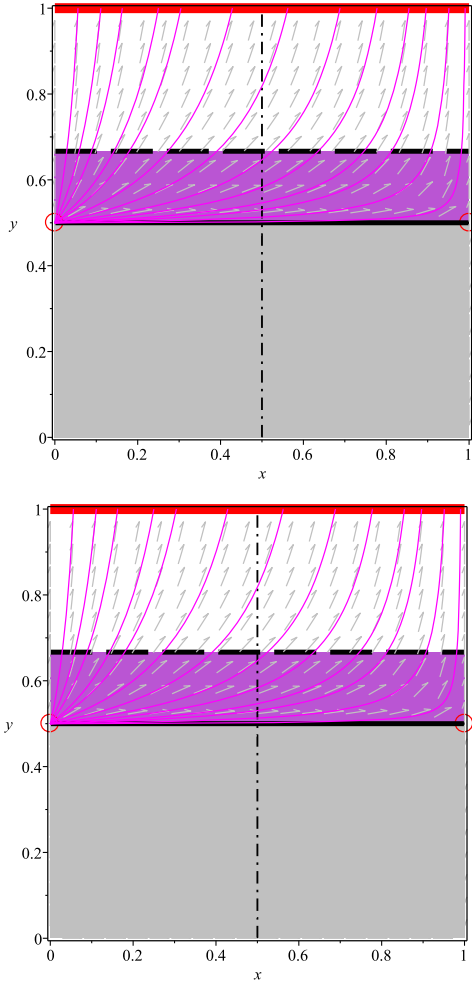


FIG. 2. Phase portrait of the dynamical systems for models 1 (top panels) and 2 (bottom panels) for the Λ CDM model: $\lambda_4 = \lambda_3 = 0$ (as before, we consider radiation with $\omega_m = 1/3$). The critical points $P_{\text{bb}} : (0, 1/2)$ and $P_{\text{mat}} : (1, 1/2)$ are enclosed by the small circles, while the de Sitter critical manifold \mathcal{M}_{ds} is represented by the thick solid horizontal (red) line coincident with the upper boundary. The vertical dash-dot straight line represents the condition $H = L^{-1}$. The solid dark curve represents the separatrix \mathcal{S} and the dark dash curve corresponds to the condition $q = -1 - \dot{H}/H^2 = 0$. The region below the separatrix (gray shading) corresponds to anti-de Sitter background space. Above the dashed curve the expansion is accelerated while below it the cosmic expansion is decelerated.

$$x_{\text{Pl}} = \frac{1}{1 + \alpha}. \quad (38)$$

Hence, the location of the Planck scale in the x direction of the phase plane is completely determined by the ratio α (35) which, as said, should be fixed by the theory. In the absence of an accurate estimate for the ratio of the new and the Planck lengths (squared), for the purposes of the numerical investigation we arbitrarily assume that $\alpha = 9$, so that $L = 3L_{\text{Pl}}$. This arbitrary value is the one used in Fig. 1.

In the classical limit $\lambda_k \rightarrow 0$, which corresponds to the formal limit $L_{\text{Pl}}^{-1} \rightarrow \infty$, the location of the quantum boundary shifts to the origin, $x_{\text{Pl}} \rightarrow 0$, so that the quantum domain disappears (see Fig. 2).

An additional comment is necessary at this point. Since it is based on the tools of the dynamical systems theory, our study is strictly qualitative so that the actual location x_{Pl} of the Planck scale in the phase square is irrelevant and so is any specific assumption on the quantitative relationship between the Planck scale and the new scales, $\alpha = L^2/L_{\text{Pl}}^2$.

Quantum fluctuations of the cosmological horizon at the Planck scale,

$$|\delta_q H^{-1}| \sim L_{\text{Pl}} \Rightarrow |\delta_q H| \sim L_{\text{Pl}}^{-1},$$

induce fluctuations of the x -position of the quantum boundary in the phase space,⁶

$$|\delta_q x| \sim \frac{2L^2/L_{\text{Pl}}^2}{(1 + L^2/L_{\text{Pl}}^2)^2} = \frac{2\alpha}{(1 + \alpha)^2}, \quad (39)$$

where the x -position of the quantum boundary is not a fixed value but an averaged quantity instead:

$$x_{\text{Pl}} = \langle x \rangle. \quad (40)$$

Hence, we get a fuzzy boundary around the average position: $\langle x \rangle \pm |\delta_q x|/2$.

A. Critical points and their properties

The critical points $P_i : (x_i, y_i)$ of the dynamical systems (18) and (30) in the physically meaningful phase spaces $\Psi_{\text{phys},1}$ and $\Psi_{\text{phys},2}$, respectively, as well as their stability properties, are listed and briefly discussed below (see Fig. 1). Recall that since both dynamical systems are mathematically equivalent—see the text below equation (30)—the asymptotic properties of the corresponding phase spaces will be qualitatively the same. This is why, in what follows, we present the critical points and/or manifolds, as well as their stability properties, in a unified way for both models.

(1) Quantum inflationary manifold,

$$\mathcal{Q}_{\text{infl}} = \{(x, 0) : 0 \leq x \leq \langle x \rangle\}, \quad (41)$$

where the length of the manifold is an averaged value. This is a “fuzzy manifold” since $\langle x \rangle$ is not a definite value but, rather, an averaged quantity because due to the quantum behavior near the Planck scale L_{Pl}^{-1} , there are quantum fluctuations. Here, and in what follows, we assume that at the average value $\langle x \rangle$, $H = L_{\text{Pl}}^{-1}$, i.e., that (40) takes place. The above

⁶See the derivation of (39) in Sec. IV B 2.

qualitative picture is legitimate since (i) in the present set up, the new and the Planck scales are in a numerical relationship of similarity: $L^{-1} \lesssim L_{\text{Pl}}^{-1}$ ($\alpha \gtrsim 1$) and (ii) our study is strictly qualitative. In Fig. 1, the curvature scale $H^2 = L^{-2}$ is represented by the dash-dot vertical straight line that splits the phase portraits into two halves. To the left of this line (left-hand half) the probed energies are greater than the new energy scale, up to the boundary of the quantum domain (vertical dark-gray strip centered at $x = \langle x \rangle$ in Fig. 1) where the Planck energy is probed.

What we have called the quantum inflationary manifold $\mathcal{Q}_{\text{infl}}$ can be found only through numeric investigation. We recall that in the quantum domain the dynamical system may not be well-defined. Nevertheless, in the understanding that the present set up may be viewed as a quantum effective theory of gravity, we may trust our computations at least up to the boundary of the quantum domain.

From the numerical investigation it follows that critical points in $\mathcal{Q}_{\text{infl}}$ are past attractors. In general the manifold is a global past attractor since any possible orbit in the phase space starts at a point in $\mathcal{Q}_{\text{infl}}$. Although in the quantum domain we lose track of any classical curve—such as, for instance, the separatrix or the curve where $q = 0$ —immediately after abandoning points in $\mathcal{Q}_{\text{infl}}$ the orbits of the phase space enter a region where the expansion is accelerated, this is why we may relate this manifold with inflationary behavior.

It is verified that several relevant quantities evaluated at points in $\mathcal{Q}_{\text{infl}}$ blow up. For instance:

$$\Omega_m \rightarrow \infty, \quad \Omega_\Lambda \rightarrow \infty. \quad (42)$$

While the first limit may be associated with $\rho_m \rightarrow \infty$ and a large but finite Hubble rate, the second limit is unphysical. Actually, even for those points in $\mathcal{Q}_{\text{infl}}$ where H^2 is very large but finite ($H^2 \geq L_{\text{Pl}}^{-2}$), the only way in which the limit $\Omega_\Lambda = \Lambda/3H^2 \rightarrow \infty$ can be attained is when the cosmological constant $\Lambda \rightarrow \infty$, which is clearly phenomenologically incorrect. This inconsistency of the classical equations of motion must be only a manifestation of the quantum nature of points in this manifold. Hence, our assumption that $\mathcal{Q}_{\text{infl}}$ may be located inside the quantum domain $H^2 > L_{\text{Pl}}^{-2}$, where the equations of motion of the present classical formalism are not supposed to be valid, is justified. The resulting qualitative picture is one where all points in the quantum manifold lie in the trans-Planckian region of the phase square. If there were some points of $\mathcal{Q}_{\text{infl}}$ in the classical domain where $H^2 < L_{\text{Pl}}^{-2}$, then there would be no feasible classical explanation to the second limit in (42).

For points located inside the trans-Planckian region, it happens that $\dot{H}/H^2 \rightarrow 0$, which means that the expansion is always de Sitter in that region of the phase square. It is seen from Fig. 1 that the orbits generated by initial data (x_{i0}, y_{i0}) inside the quantum domain (vertical dark-gray strip in Fig. 1) are almost vertical straight lines ($x \approx x_{i0} \Rightarrow H \approx H_{i0}$), which means that the corresponding cosmological evolution is an everlasting de Sitter expansion. For these cosmic histories there is not low-energy physics; the classical domain $H^2 < L^{-2}$ is never attained. Hence, no phenomenologically viable cosmological dynamics are possible. Only in orbits that have originated from initial conditions either in the neighborhood or outside of the quantum domain it is possible to scape to the classical region and to produce, accordingly, viable phenomenological cosmic dynamics. Yet, if we evolve these phenomenologically viable orbits back into the trans-Planckian region of phase space, the numeric investigation shows that these originate from the right edge of the quantum manifold. Hence, every possible orbit, no matter whether it could be associated with viable phenomenological dynamics or not, is originated at the past attractor manifold $\mathcal{Q}_{\text{infl}}$.

- (2) Standard big bang solution $P_{\text{bb}} : (0, 1/2)$. In this case $x = 0 \Rightarrow H \gg L^{-1}$, while $y = 1/2 \Rightarrow \Omega_m = 1$. This solution exists only for $\lambda_k = 0$, i.e., in the classical limit of models 1 and 2, where the higher curvature corrections to gravity are vanishing and the quantum domain disappears. Whenever it exists, P_{bb} is the global past attractor (see Fig. 2).
- (3) Matter domination, $P_{\text{mat}} : (1, 1/2) \Rightarrow H \ll L^{-1}$ and $\Omega_m = 1$, i.e., $3H^2 = \rho_m$. Given that the eigenvalues of the linearization matrix at P_{mat} ,

$$\lambda_1 = -3(\omega_m + 1)/2, \quad \lambda_2 = 3(\omega_m + 1)/2,$$

are of different sign, this means that the matter-dominated solution is a saddle critical point. At this solution $\Omega_\Lambda = 0$, while $\Omega_m = 1 \Rightarrow 3H^2 = \rho_m$ and

$$\frac{\dot{H}}{H^2} = -\frac{3}{2}(\omega_m + 1) \Rightarrow q = \frac{3\omega_m + 1}{2}.$$

- (4) The de Sitter attractor manifold,

$$\mathcal{M}_{\text{ds}} = \{(x, 1) : 0 \leq x \leq 1\}, \quad (43)$$

which exists only for de Sitter ($\Lambda > 0$) background spaces. For points in \mathcal{M}_{ds} we obtain the following eigenvalues of the corresponding linearization matrix: $\lambda_1 = 0$, $\lambda_2 = -3(\omega_m + 1)$. The vanishing eigenvalue is associated with an eigenvector that is tangent to the manifold at each point. The second eigenvalue is always a negative quantity. This means

that, as seen from Fig. 1, each one of the critical points in \mathcal{M}_{dS} is a local attractor, i.e., the manifold itself is a global attractor of orbits in Ψ . For each point in the de Sitter attractor manifold, $\dot{H} = 0$, $\Omega_m = 0 \Rightarrow q = -1$. Besides,

$$\Omega_\Lambda = 1 + \lambda_4 \left(\frac{1-x_0}{x_0} \right)^3 e^{\left(\frac{1-x_0}{x_0} \right)^2}, \quad (44)$$

for model 1, while for model 2

$$\Omega_\Lambda = 1 - \lambda_3 \left(\frac{1-x_0}{x_0} \right)^2 \left[1 - \left(\frac{1-x_0}{x_0} \right) e^{\frac{1-x_0}{x_0}} \right], \quad (45)$$

with fixed $x_0 \in \mathcal{M}_{\text{dS}}$ in both cases.

As already mentioned, due to the equivalence of the dynamical systems (18) and (30), all of the above critical sets are common to both models 1 and 2. There are not other equilibrium states in the phase spaces of these models.

B. Physical analysis of the phase portrait

The phase portraits of the dynamical systems (18) and (30), for toy models 1 (top panels) and 2 (bottom panels), respectively, are shown in Fig. 1. The critical point P_{mat} appears enclosed by the small circles, while the de Sitter attractor manifold \mathcal{M}_{dS} is represented by the thick horizontal (red) line joining the points (0, 1) and (1, 1), i.e., this manifold coincides with the upper boundary of the phase square. The inflationary quantum manifold $\mathcal{Q}_{\text{infl}}$ is represented by the thick horizontal (red) segment with the coordinate $y = 0$, starting at the origin and ending up at the solid circle at $\langle x \rangle$ (it coincides with the corresponding segment of the lower boundary). As a matter of fact $\langle x \rangle$ is an averaged value due to quantum fluctuations $\delta_q x$ of the boundary of the inflationary manifold [see Eq. (39)]. The value $\langle x \rangle$ defines the condition $H = L_{\text{pl}}^{-1}$ (thick vertical long-dash red line in Fig. 1), i.e., it represents the average value of the fuzzy boundary of the quantum domain (thickness $\delta_q x$) behind which the equations of the present formalism are not valid anymore. The vertical straight dash-dot line represents the x -position where $H = L^{-1}$. To the left of this line the energies are higher than the new scale L^{-1} .

For completeness, the relevant curves $\bar{y}_j = \bar{y}_j(x)$ ($j = 1$ for model 1, while $j = 2$ for model 2) in (22) and (32), respectively, i.e., the separatrices represented by the solid dark curves in the figure, and $\hat{y}_j = \hat{y}_j(x)$ in (25) and (34) (dashed dark curves), respectively, have been included as well in the phase portraits. The region below the separatrix (gray shading) corresponding to anti-de Sitter background spaces is not of interest for the present investigation. The region with $\bar{y}_j \leq y \leq \hat{y}_j$ (magenta shading in the figure) is

where the expansion is decelerated and cosmic structure may form.

I. Λ CDM model

The existence of the energy scale $L^{-1} \lesssim L_{\text{pl}}^{-1}$ appreciably modifies the global dynamics of the Λ cold dark matter (Λ CDM) model emerging from the geometric inflation formalism when compared with the known GR-based result. Actually, the Λ CDM model retrieved from the present set up in the limit when the coupling $\lambda_k \rightarrow 0$ (see Fig. 2) does not exactly coincide with the one obtained within the GR framework. In this limit the quantum manifold $\mathcal{Q}_{\text{infl}}$ is replaced by the global past attractor $P_{\text{bb}}: (0, 1/2)$, which is associated with a matter dominated ($\Omega_m = 1$) big bang ($H^2 \rightarrow \infty$), while the matter dominated saddle point $P_{\text{mat}}: (1, 1/2)$, where $\Omega_m = 1$ and $H^2 \ll L^{-2}$, and the de Sitter manifold \mathcal{M}_{dS} (the global future attractor) are also critical states of the model.⁷ Meanwhile, in the GR-based Λ CDM model, where $\Omega_m + \Omega_\Lambda = 1$, a one-dimensional dynamical system is obtained which is driven by the following ordinary differential equation:

$$\dot{\Omega}'_m = 3(\omega_m + 1)\Omega_m(\Omega_m - 1). \quad (46)$$

As seen in this case, only two critical points can be found: (i) the matter-dominated ($\Omega_m = 1$) past attractor, and (ii) the de Sitter future attractor with $\Omega_m = 0$.

This discrepancy may be due to the fact that, for the GR-based Λ CDM model, since there is not any intrinsic energy scale, the matter-dominated solution, $\Omega_m = 1 \Rightarrow 3H^2 = \rho_m$, comprises both cases—the big bang singularity when $H^2 \rightarrow \infty$ and $\rho_m \rightarrow \infty$, as well as any other stage of matter dominance, when both H and ρ_m are finite. The problem here is that since the matter-dominated solution is the past attractor, one has to decide whether to put the origin of the cosmic history at the big bang (singular) event or at a matter-dominated stage with the finite curvature and energy density that is necessary to generate the amount of observed cosmic structure. This is to be contrasted with the Λ CDM limit of the geometric inflation model where, since there exists an intrinsic energy scale L^{-2} , the big bang event (P_{bb}) and the matter-dominated stage with finite energy density (P_{mat}) are differentiated according to whether $H^2 \gg L^{-2}$ (big bang) or $H^2 \ll L^{-2}$ (matter dominance necessary for the structure formation). In this case the big bang is the starting point of any potential cosmic history, while the matter-dominated stage that allows for the formation of cosmic structure is a transient stage, as required by the standard cosmic paradigm. The GR-based Λ CDM model

⁷The limit $\lambda_k \rightarrow 0$ is equivalent to the “classical limit” $L_{\text{pl}} \rightarrow 0$. Hence, this may be thought of as the classical limit of the geometric inflation formalism where the quantum effects are neglected. Even in this classic limit the existence of the scale L^{-1} makes a difference as compared with GR.

can be recovered from the geometric inflation set up in the limit $LH \rightarrow 0$, instead of $\lambda_k \rightarrow 0$.

It is worth noticing that the Λ CDM limit of the geometric inflation formalism, where the quantum domain is shrunk to the neighborhood of the point $x = 0$, is a classic limit in the sense that the coupling λ_k of the higher-order curvature contributions to gravity is vanishing. This means that any geometrical manifestation of the quantum effects is eliminated—as seen from Fig. 2, the quantum domain is not visible—and the big bang singularity appears in its place.

2. Quantum inflationary manifold $\mathcal{Q}_{\text{infl}}$

As said before, this is a fuzzy manifold which completely lies within the quantum domain $H \geq L_{\text{pl}}^{-1}$. Along the manifold, from $x = 0$ to $x = \langle x \rangle$, the Hubble parameter changes from a very high curvature regime $H \gg L_{\text{pl}}^{-1}$ at $x = 0$, to

$$H(\langle x \rangle) = \sqrt{\frac{1 - \langle x \rangle}{\langle x \rangle}} L^{-1}, \quad (47)$$

at $x = \langle x \rangle$. In this paper, we identify the average value $\langle x \rangle$ with the mean x -position of the Planck scale: $H = L_{\text{pl}}^{-1}$. In Fig. 1, $\langle x \rangle$ is marked by the solid circle and the corresponding region of phase space is represented by a thick vertical long-dash (red) line. Given the qualitative nature of our present study, the precise value of $\langle x \rangle$ is irrelevant.

According to (47) at the Planck scale [compare with (37)],

$$L_{\text{pl}}^{-1} = \sqrt{\frac{1 - \langle x \rangle}{\langle x \rangle}} L^{-1} = \sqrt{\alpha} L^{-1}.$$

Hence, for the ratio $\alpha = L^2/L_{\text{pl}}^2$, we get

$$\alpha = \frac{1 - \langle x \rangle}{\langle x \rangle} \Rightarrow \langle x \rangle = \frac{1}{1 + \alpha}, \quad (48)$$

so that the average position of the quantum boundary is completely specified by the ratio α which, in turn, should be fixed by the theory (8) itself.

In order to estimate the size of the quantum fluctuations of the quantum boundary at $\langle x \rangle$, the starting point may be the definition of the x -coordinate of the phase space (36). Hence,

$$\delta x = -\frac{2L^2 H \delta H}{(1 + L^2 H^2)^2},$$

and if we define the quantum fluctuations around $\langle x \rangle$ in the following way:

$$|\delta_q x| \sim |\delta x|_{H=L_{\text{pl}}^{-1}} = \frac{2 \frac{L^2}{L_{\text{pl}}} |\delta L_{\text{pl}}^{-1}|}{(1 + \frac{L^2}{L_{\text{pl}}^2})^2} = \frac{2 \frac{L^2}{L_{\text{pl}}^2} \frac{|\delta L_{\text{pl}}|}{L_{\text{pl}}}}{(1 + \frac{L^2}{L_{\text{pl}}^2})^2}, \quad (49)$$

where in the last equation we have taken into account that $|\delta L_{\text{pl}}^{-1}| = L_{\text{pl}}^{-2} |\delta L_{\text{pl}}|$, then equation (39) is obtained from (49) by assuming that $|\delta L_{\text{pl}}| \sim L_{\text{pl}}$. By substituting $L^2 = \alpha L_{\text{pl}}^2$ and (48) into (39) one finally gets

$$|\delta_q x| \sim \frac{2\alpha}{(1 + \alpha)^2} = 2\langle x \rangle(1 - \langle x \rangle). \quad (50)$$

This means that both the “thickness” of the quantum boundary $\sim |\delta_q x|$ and its average position $\langle x \rangle$ are fixed by the assumed value of $\alpha = L^2/L_{\text{pl}}^2$. Recall that, since our study is merely qualitative, the exact value of the average position $\langle x \rangle$ is not actually relevant. In our study we have arbitrarily chosen $\alpha = 9$.

It is interesting to note that orbits that originate inside the trans-Planckian region, and in its neighborhood, are (almost) vertical lines joining a point in $\mathcal{Q}_{\text{infl}}$ with a point with (almost) the same x -coordinate in the attractor de Sitter manifold \mathcal{M}_{dS} . This means that initial conditions within the quantum domain lead to de Sitter ever expanding universes with the constant

$$H = H_0 = \sqrt{\frac{1 - x_0}{x_0}} L^{-1},$$

where $x = x_0$ is the initial condition. These are trans-Planckian ever-inflating universes. We have to recall, however, that inside the quantum domain we may not trust the results obtained on the basis of the present classical theory.

In order for a given orbit to lead to sensible cosmic dynamics, it should leave the quantum domain and after a primordial inflationary period, meet the region of the phase space where the expansion occurs at a decelerated pace ($q > 0$); the region below the curve where $q = 0$ (dashed curve in Fig. 1) and above the separatrix (solid curve), i.e., the region where $\bar{y}_j(x) \leq y < \hat{y}_j(x)$, with $\bar{y}_j(x)$, and $\hat{y}_j(x)$ ($j = 1, 2$) given by (22), (32) and (25), (34), respectively (magenta shaded region in the phase portrait). In Fig. 1 the orbits that lead to well-behaved cosmic dynamics are the same color of the region where the deceleration parameter $q > 0$ (magenta shaded region). The decelerated expansion stage is mandatory for the required amount of cosmic structure to form. For those orbits that always evolve in the region where the expansion is accelerated, no cosmic structure forms at all.

3. De Sitter attractor manifold \mathcal{M}_{dS}

The de Sitter attractor manifold owes its existence to the nonvanishing cosmological constant Λ that is included in

the model from the start [17]. This warrants that the decelerated expansion, whenever it takes place, can be only a transient stage of the cosmic evolution. From Fig. 1 it is seen that those orbits that represent sensible cosmic dynamics start in a stage of primordial curvature inflation, then go into a stage of decelerated expansion where the appropriate amount of cosmic structure forms (magenta-shaded region in Fig. 1), to finally enter another inflationary stage and, eventually, to end up in a de Sitter regime.

V. DISCUSSION

There are two inflationary stages in the geometric inflation model. One primordial inflationary period and a second inflationary stage at late times. For some orbits—those leading to sterile evolution, i.e., without formation of cosmic structure—these stages are continuously joined, while others that allow for the correct amount of cosmic structure to form have an intermediate epoch of decelerated expansion which joins the two inflationary stages (see Fig. 1). Hence, the arising of sensible cosmological dynamics in the geometric inflation model depends on the initial conditions.

From the motion Eqs. (13) and (26), it follows that

$$-2\dot{H} = \frac{(w_m + 1)\rho_m}{1 + 2\lambda_4(2 + L^4 H^4)L^6 H^6 e^{L^4 H^4}}, \quad (51)$$

for model 1, while

$$-2\dot{H} = \frac{(w_m + 1)\rho_m}{1 - 3\lambda_3 L^4 H^4 + \lambda_3(4 + L^2 H^2)L^6 H^6 e^{L^2 H^2}}, \quad (52)$$

for model 2, where $\rho_m \propto a^{-3(w_m+1)}$. In the very high curvature limit $H \gg L^{-1}$, the de Sitter expansion is approached as long as

$$L^{10} H^{10} e^{L^4 H^4} \gg a^{-3(w_m+1)},$$

for model 1 or

$$L^8 H^8 e^{L^2 H^2} \gg a^{-3(w_m+1)},$$

for model 2, so that $\dot{H} \rightarrow 0$. The very high curvature regime $H \gg L_{\text{Pl}}^{-1}$ falls in the quantum domain where the motion equations of the geometric inflation model stop being valid. Hence, while at late times the expansion is de Sitter $a(t) \propto \exp(\sqrt{\Lambda/3}t)$, at early times the inflationary stage is not always de Sitter. As we have just shown, the primordial de Sitter inflation takes place in the quantum domain (vertical orbits in the dark-gray strip in Fig. 1) so that no sensible cosmic dynamics can be linked with it.

The sensible cosmological scenario in the present formalism takes place if for cosmic evolution in the part of the phase square in Fig. 1 to the left of the vertical

dash-dot line and up to the boundary of the quantum domain ($L^{-2} \lesssim H^2 \lesssim L_{\text{Pl}}^{-2}$), the crossing of the condition $q = 0$ in the direction from $q < 0$ to $q > 0$ is possible. For the choice $w_m = 1/3$ (background radiation) at early times where $\rho_m \gg \Lambda$, the deceleration parameter $q = -1 - \dot{H}/H^2$ reads⁸:

$$q = \frac{1 - 2\lambda_4(1 + L^4 H^4)L^6 H^6 e^{L^4 H^4}}{1 + 2\lambda_4(2 + L^4 H^4)L^6 H^6 e^{L^4 H^4}}, \quad (53)$$

for model 1, while for model 2 we have

$$q = \frac{1 + \lambda_3 L^4 H^4 - \lambda_3(2 + L^2 H^2)L^6 H^6 e^{L^2 H^2}}{1 - 3\lambda_3 L^4 H^4 + \lambda_3(4 + L^2 H^2)L^6 H^6 e^{L^2 H^2}}. \quad (54)$$

Hence, the condition $q = 0$ amounts to

$$(1 + L^4 H^4)L^6 H^6 e^{L^4 H^4} = \frac{1}{2\lambda_4}, \quad (55)$$

for model 1 and

$$(2 + L^2 H^2)L^6 H^6 e^{L^2 H^2} = \frac{1}{\lambda_3} + L^4 H^4, \quad (56)$$

for model 2. Whenever the left-hand side (LHS) in the above equations is greater than the right-hand side (RHS), recalling that $L^{-1} \lesssim H \lesssim L_{\text{Pl}}^{-1}$, primordial non-de Sitter inflation takes place. Then, as long as H further decreases so that the LHS of Eqs. (55) and (56) becomes smaller than the RHS, the crossing of the condition $q = 0$ takes place and the corresponding phase space orbits enter a decelerated expansion region (magenta shading in Fig. 1), with the consequent formation of cosmic structure.

Finally, let us discuss on another important aspect of the present effective theory. Classical GR must be, at most, the infrared limit of some quantum gravity theory. This means that modifications of general relativity with the inclusion of low-energy quantum corrections must be seen as an effective quantum theory of the gravitational interactions [34]. For example, the low-energy string effective action can be seen, at tree-level, as a perturbative expansion in powers of the Regge slope. This expansion yields, in addition to the Einstein action, corrections that are quadratic and higher-order in the curvature [42]. Several of the coefficients of the expansion may be uniquely fixed by comparing string-theory and field-theory S-matrices [38–42]. However, those coefficients of the expansion, which change under field redefinitions in the effective action

⁸Notice from Eqs. (53) and (54) that if we consider the very high curvature regime $H^2 \gg L^{-2}$, it follows that $q \rightarrow -1$, i.e., this is a de Sitter expansion regime taking place in the quantum domain $H^{-1} < L_{\text{Pl}}$, as discussed above.

that, according to the equivalence theorem [43–46], leave the S-matrix unchanged, are ambiguous [20,38,47].

As discussed in Sec. II in the paragraph below Eq. (10) (see the related discussion in [17]), the above ambiguity also affects other kinds of effective theory like the one of our interest in this paper (8). What can we learn from the results of our study in regards to the mentioned ambiguity? Here we have shown [see the paragraph below Eq. (30)] that the dynamical systems (18) (model 1) and (30) (model 2) are mathematically equivalent under the transformation (31). This entails that the global dynamics that follow from the corresponding phase portraits are essentially (qualitatively) the same. This is clearly illustrated in Fig. 1. On the other hand, both models 1 and 2 are based on different choices of the dimensionless constants λ_n in the expansion of the effective action (8). Model 1—given by (11)—is due to the following choice: $\lambda_{2k+1} = 0$, $\lambda_{4+2k} = \lambda_4/k!$ (k is a positive integer). Model 2—given by (12)—is obtained after the choice $\lambda_3 > 0$, $\lambda_{n \geq 4} = (-1)^n \lambda_3 / (n-4)!$. The fact that these quite unrelated choices of the coefficients of the expansion in the higher-curvature invariants lead to qualitatively the same global dynamics may be seen as an indication that the ambiguity discussed above bears no relevance to the asymptotic properties of the models. However, we do not know how this result may affect the similar ambiguity issue found in the string theory framework. This latter issue deserves separate investigation.

VI. CONCLUSION

In this paper the geometric origin of primordial inflation in the geometric inflation formalism [17] has been investigated on the basis of the dynamical systems analysis for the first time. We have studied two toy models proposed in the mentioned reference, where the sum over the infinite tower of higher-order curvature invariants is performed, yielding to compact expressions in the equations of motion. These are very encouraging possibilities if we regard gravity as a quantum effective theory [34], since higher powers of R , $R_{\mu\nu}$, and $R_{\mu\nu\sigma\lambda}$ would be involved at higher loops. Hence, one would naively expect that consideration of the whole infinite tower of curvature invariants would amount to consideration of all of the higher-order loops, so that quantum effects would be manifested.

Perhaps the more interesting result of the present research has been to show, precisely, the quantum origin of the primordial inflation in the geometric inflation theory. This is a consequence of the new length scale L which is assumed above (but not too much) of the Planck length L_{Pl} :

$L \gtrsim L_{\text{Pl}}$. As seen from Fig. 1, for equilibrium points in the inflationary past attractor we have that $H^{-1} < L_{\text{Pl}}$, so that every orbit, no matter whether it leads to unphysical or phenomenologically viable cosmic dynamics, starts in the past attractor within the quantum domain.

In a recent paper [32], the global dynamics of an up-to-cubic curvature correction to GR, known as “cosmological Einsteinian cubic gravity,” were explored. The results of that paper show that the asymptotic cosmological dynamics are qualitatively similar to the one of the classical Λ CDM limit of the geometric inflation model ($\lambda_k \rightarrow 0$). In this regard, compare the left panel of Fig. 1 of [32] with Fig. 2 of this paper, noticing that a different set of phase space variables were used in the former study. In the mentioned reference, the matter-dominated big bang is the global past attractor instead of the quantum manifold found in this paper, where the whole infinite tower of higher-order curvature corrections to GR is considered. We may explain the qualitative differences between both studies by arguing precisely that, while here we have considered toy models that included the infinite tower of higher curvature invariants, in [32] only terms up to cubic order were included. We think that these are not enough to excite quantum effects.

In order to allow for under-Planckian initial energy densities, recently a hybrid geometric inflation model was proposed [48], where the role of a scalar field in the geometric inflation formalism is investigated. Although this model misses one of the most attractive features of the geometric inflation formalism, the pure geometrical origin of primordial inflation, it would be very interesting to explore the asymptotic dynamics of such a hybrid scenario. This will be the subject of forthcoming work.

ACKNOWLEDGMENTS

The authors are grateful to FORDECYT-PRONACES-CONACYT for support of the present research under Grant No. CF-MG-2558591. The work of R. G. S. was partially supported by Secretaría de Investigación y Posgrado Grants No. SIP20200666 and No. SIP20210500, Comisión de Operación y Fomento de Actividades Académicas COFAA-IPN, and Estímulo al Desempeño a la Investigación EDI-IPN. F. X. L. C. also acknowledges the Programa para el Desarrollo Profesional Docente (PRODEP) for financial support and the receipt of the Grant from the Abdus Salam International Centre for Theoretical Physics, Trieste, Italy. U. N. thanks PRODEP-SEP and CIC-UMSNH for financial support of his contribution to the present research.

- [1] R. Utiyama and B. S. DeWitt, *J. Math. Phys. (N.Y.)* **3**, 608 (1962).
- [2] G. 't Hooft and M. J. G. Veltman, *Ann. Inst. H. Poincaré Phys. Theor. A* **20**, 69 (1974).
- [3] B. S. DeWitt, *Phys. Rep.* **19**, 295 (1975).
- [4] K. S. Stelle, *Phys. Rev. D* **16**, 953 (1977).
- [5] K. S. Stelle, *Gen. Relativ. Gravit.* **9**, 353 (1978).
- [6] A. Hindawi, B. A. Ovrut, and D. Waldram, *Phys. Rev. D* **53**, 5583 (1996).
- [7] A. Hindawi, B. A. Ovrut, and D. Waldram, *Phys. Rev. D* **53**, 5597 (1996).
- [8] D. Lovelock, *J. Math. Phys. (N.Y.)* **12**, 498 (1971).
- [9] D. Lovelock, *J. Math. Phys. (N.Y.)* **13**, 874 (1972).
- [10] T. Clifton, P. G. Ferreira, A. Padilla, and C. Skordis, *Phys. Rep.* **513**, 1 (2012).
- [11] P. Bueno and P. A. Cano, *Phys. Rev. D* **94**, 104005 (2016).
- [12] P. Bueno and P. A. Cano, *Phys. Rev. D* **94**, 124051 (2016).
- [13] R. A. Hennigar, D. Kubiznak, and R. B. Mann, *Phys. Rev. D* **95**, 104042 (2017).
- [14] X. H. Feng, H. Huang, S. L. Li, H. Lu, and H. Wei, *Eur. Phys. J. C* **80**, 1079 (2020).
- [15] G. Arciniega, J. D. Edelstein, and L. G. Jaime, *Phys. Lett. B* **802**, 135272 (2020).
- [16] A. Cisterna, N. Grandi, and J. Oliva, *Phys. Lett. B* **805**, 135435 (2020).
- [17] G. Arciniega, P. Bueno, P. A. Cano, J. D. Edelstein, R. A. Hennigar, and L. G. Jaime, *Phys. Lett. B* **802**, 135242 (2020).
- [18] M. C. Pookkillath, A. De Felice, and A. A. Starobinsky, *J. Cosmol. Astropart. Phys.* **07** (2020) 041.
- [19] M. C. Bento and O. Bertolami, *Phys. Lett. B* **368**, 198 (1996).
- [20] D. J. Gross and E. Witten, *Nucl. Phys.* **B277**, 1 (1986).
- [21] J. Wainwright and G. F. R. Ellis, *Dynamical Systems in Cosmology* (Cambridge University Press, Cambridge, England, 1997).
- [22] A. A. Coley, *Dynamical Systems and Cosmology* (Dordrecht-Kluwer, Netherlands, 2003).
- [23] E. J. Copeland, A. R. Liddle, and D. Wands, *Phys. Rev. D* **57**, 4686 (1998).
- [24] V. Faraoni and C. S. Protheroe, *Gen. Relativ. Gravit.* **45**, 103 (2013).
- [25] S. Bahamonde, C. G. Bohmer, S. Carloni, E. J. Copeland, W. Fang, and N. Tamanini, *Phys. Rep.* **775–777**, 1 (2018).
- [26] I. Quiros, *Int. J. Mod. Phys. D* **28**, 1930012 (2019).
- [27] R. García-Salcedo, T. Gonzalez, F. A. Horta-Rangel, I. Quiros, and D. Sanchez-Guzmán, *Eur. J. Phys.* **36**, 025008 (2015).
- [28] A. Avelino, R. García-Salcedo, T. Gonzalez, U. Nucamendi, and I. Quiros, *J. Cosmol. Astropart. Phys.* **08** (2013) 012.
- [29] R. García-Salcedo, T. Gonzalez, I. Quiros, and M. Thompson-Montero, *Phys. Rev. D* **88**, 043008 (2013).
- [30] O. Obregon and I. Quiros, *Phys. Rev. D* **84**, 044005 (2011).
- [31] R. García-Salcedo, T. Gonzalez, C. Moreno, Y. Napoles, Y. Leyva, and I. Quiros, *J. Cosmol. Astropart. Phys.* **02** (2010) 027.
- [32] I. Quiros, R. García-Salcedo, T. Gonzalez, J. L. Morales Martínez, and U. Nucamendi, *Phys. Rev. D* **102**, 044018 (2020).
- [33] M. Marciu, *Phys. Rev. D* **101**, 103534 (2020).
- [34] J. F. Donoghue, *Phys. Rev. D* **50**, 3874 (1994).
- [35] M. H. Goroff and A. Sagnotti, *Nucl. Phys.* **B266**, 709 (1986).
- [36] X. O. Camanho, J. D. Edelstein, J. Maldacena, and A. Zhiboedov, *J. High Energy Phys.* **02** (2016) 020.
- [37] D. G. Boulware and S. Deser, *Phys. Lett. B* **175**, 409 (1986).
- [38] A. A. Tseytlin, *Phys. Lett. B* **176**, 92 (1986).
- [39] R. R. Metsaev and A. A. Tseytlin, *Nucl. Phys.* **B293**, 385 (1987).
- [40] R. R. Metsaev and A. A. Tseytlin, *Phys. Lett. B* **185**, 52 (1987).
- [41] M. C. Bento and N. E. Mavromatos, *Phys. Lett. B* **190**, 105 (1987).
- [42] M. C. Bento and O. Bertolami, *Phys. Lett. B* **228**, 348 (1989).
- [43] E. C. Nelson, *Phys. Rev.* **60**, 830 (1941).
- [44] F. J. Dyson, *Phys. Rev.* **73**, 929 (1948).
- [45] A. Salam and J. A. Strathdee, *Phys. Rev. D* **2**, 2869 (1970).
- [46] M. C. Bergere and Y. M. P. Lam, *Phys. Rev. D* **13**, 3247 (1976).
- [47] S. Deser and A. N. Redlich, *Phys. Lett. B* **176**, 350 (1986).
- [48] J. D. Edelstein, D. Vázquez Rodríguez, and A. Vilar López, *J. Cosmol. Astropart. Phys.* **12** (2020) 040.